

The Puromycin Route to Assess Stereo- and Regiochemical Constraints on Peptide Bond Formation in Eukaryotic Ribosomes

Shelley R. Starck, Xin Qi, Brett N. Olsen, and Richard W. Roberts*

Division of Chemistry and Chemical Engineering, California Institute of Technology, Pasadena, California 91125

Received February 22, 2003; E-mail: roberts@caltech.edu

The protein synthesis machinery can be used to incorporate unnatural amino acids into peptides,¹ proteins,² and molecular libraries³ (see ref 4 for reviews). These studies indicate that the ribosome displays a broad ability to utilize residues beyond the 20 naturally occurring amino acids. Chemically misacylated tRNA fragments and tRNAs have provided one route to probe the stereo- and regiochemical constraints of isolated ribosomes⁵ and intact translation systems.^{4b,6} This approach has expanded our understanding of the range of residues incorporated by the ribosome.⁷ However, entry of both β - and D-amino acids has proved challenging.^{1b,2a,5} Analysis of these residues would deepen our understanding of the stereo- and regiochemical constraints of ribosome-mediated peptide bond formation.

Here, we have used a series of synthetic puromycin analogues to measure the activity of both β - and D-amino acids in an intact eukaryotic translation system. Puromycin is a small-molecule mimic of aminoacyl-tRNA (aa-tRNA), and acts as a universal translation inhibitor by entering the ribosomal A site and participating in peptide bond formation with the nascent peptidyl chain.⁸ Puromycin and puromycin analogues have been very useful in exploring the activity of nucleophiles ($-\text{OH}$ vs $-\text{NH}_2$ vs $-\text{SH}$) in peptide bond formation and the structural requirements for inhibition of translation.⁹ Unlike aa-tRNA, puromycin is able to enter the ribosome independently, does not induce EF-Tu·GTPase activity,¹⁰ and does not require soluble translation factors for function.¹¹ Puromycin and related compounds therefore provide a direct means to address ribosome-mediated peptide bond formation in the context of a fully competent translation extract.

We synthesized a series of puromycin derivatives (Figure 1) that differ in the (1) amino acid moiety, (2) amino acid stereochemistry, and (3) number of carbon units in the amino acid backbone. We then measured the activity of each compound (Figure 2) in a high dynamic-range IC_{50} potency assay using the rabbit reticulocyte protein synthesis system.¹¹ The naturally occurring compound, L-puromycin (**1a**), inhibits globin mRNA translation with an IC_{50} of $1.8 \mu\text{M}$ (Figure 2). Surprisingly, D-puromycin (**1b**) also inhibited translation giving an IC_{50} of $280 \mu\text{M}$ (Figure 2), a difference of 150-fold.

We reasoned that stereoselectivity should be a function of the side-chain size and geometry. To test this, we constructed compounds where the puromycin side chain was altered to bear either a bulky (L- or D-4-methyl-phenylalanine; **2a** and **2b**), or a small substituent (L- or D-alanine; **3a** and **3b**). Compound **2a** inhibits translation better than puromycin itself ($\text{IC}_{50} = 1.0 \mu\text{M}$; Figure 2C) and is the most potent compound we constructed. The D-amino acid variant (**2b**) shows much lower activity ($\text{IC}_{50} = 2400 \mu\text{M}$), is ~ 9 -fold lower than D-puromycin (**1b**), and is 2400-fold less potent than the L-isomer. The alanine analogues ($\text{R} = \text{CH}_3$) show only 3-fold selectivity for the L- versus D- isomers (**3a** vs **3b**; Figure 2C). These observations argue that ribosomal stereoselectivity falls

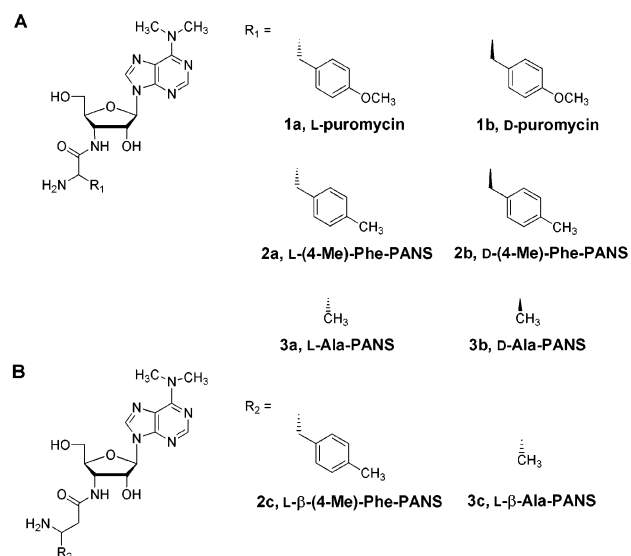


Figure 1. Puromycin analogues with (A) L- and D- α -amino acid side chains and (B) L- β -amino acid side chains.

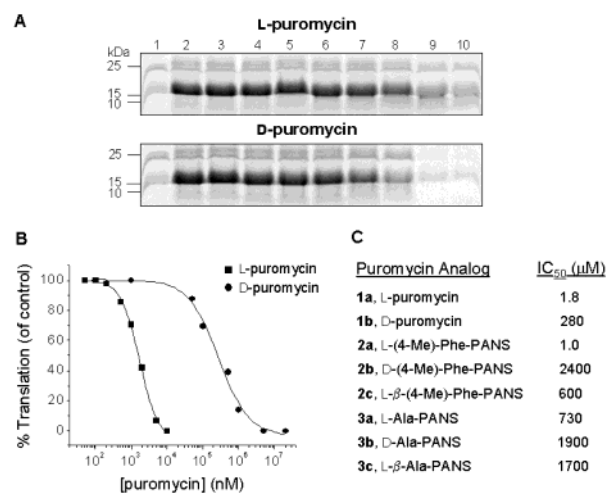


Figure 2. IC_{50} determination for puromycin and puromycin analogues, **1a–3c**. (A) Tricine-SDS-PAGE analysis of $[^{35}\text{S}]\text{Met}$ -globin translation reactions in the presence of L-puromycin (**1a**) and D-puromycin (**1b**): Lane 1, no template; lane 2, globin alone; lanes 3–10, concentrations from 50 nM to 10 mM for **1a** and from 100 nM to 20 mM for **1b**. (B) Percent globin translation relative to the globin only control for L-puromycin (**1a**) and D-puromycin (**1b**). (C) IC_{50} values for puromycin analogues **1a–3c**.

over a broad range and is primarily dictated by the size and geometry of the pendant side chain. Within the L-amino acid series (**1a**, **2a**, and **3a**), marked variation is also seen based solely on side chain identity. Larger, hydrophobic side chains provide improved function, consistent with previous observations.^{9c–d} In the D-amino acid series, the 4-O-methyltyrosine derivative (**1b**)

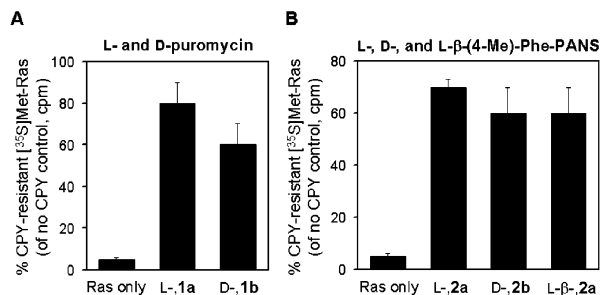


Figure 3. Carboxypeptidase Y (CPY) analysis of protein–puromycin products.¹¹ TCA precipitation of [³⁵S]Met-protein (Ras) from translation reactions after CPY treatment containing (A) Ras only, L-puromycin (**1a**) at 2 μM, and D-puromycin (**1b**) at 500 μM and (B) Ras only, L-(4-Me)-Phe-PANS (**2a**) at 1 μM, D-(4-Me)-Phe-PANS (**2b**) at 1500 μM, and L-β-(4-Me)-Phe-PANS (**2c**) at 1000 μM. Data represent the mean ± standard error for at least three independent experiments.

functions the best overall, and has ~3-fold better activity than the natural L-alanine variant (**3a**).

We next examined puromycin derivatives bearing β-amino acids. β-Amino acids have been previously incorporated at low levels using nonsense suppression techniques.^{1c,2a} In our experiments, both L-β-(4-Me)-Phe-PANS (**2c**) and L-β-Ala-PANS (**3c**) were able to fully inhibit translation (IC₅₀ = 600 and 1700 μM, respectively).

Finally, we wished to confirm that our puromycin analogues participated in peptide bond formation within the ribosome. Incorporation of puromycin blocks the C terminus, rendering the protein carboxypeptidase resistant.⁸ Previous work in our laboratory demonstrated that covalent puromycin incorporation is most efficient near the IC₅₀ value.¹¹ Consistent with this observation, protein synthesis performed in the presence of our puromycin derivatives near the IC₅₀ resulted in a 12- to 16-fold increase in carboxypeptidase Y (CPY)-resistant protein compared with the no-drug control (Figure 3, A and B). All derivatives also produce truncated protein fragments, consistent with entry and attachment both internally and at the end of the template (Supporting Information, Figure S1).¹¹

The structural basis for stereoselectivity in rabbit ribosomes cannot be addressed presently, as there are no high-resolution structures available. However, modeling D-puromycin (**1b**) into the active site of the *Haloarcula marismortui* 50S subunit¹² is consistent with the idea that steric effects play a role in chiral discrimination. In the atomic resolution structure, U2620 (U2585 *E. coli*) is the closest nucleotide to the D-side chain (see model in Supporting Information). Also, while many of the ribosome active-site nucleotides are highly conserved, the fact that critical residues can be mutated,¹³ implies that construction of ribosomes with altered stereo- and regiospecificity may be possible.

Our data lead us to conclude that L-, D-, and β-amino acids can participate in ribosome-mediated peptide bond formation when constructed as analogues of puromycin. This route allows us to rank both natural and unnatural residues as substrates in a physiologically complete protein-synthesizing system. Analysis using intact systems is important as reconstituted or purified systems

that are incapable of synthesizing proteins can produce markedly different results.^{4b,11,14} The data here provide one metric of the chiral and regiospecificity of mammalian ribosomes. We are hopeful that this approach, along with other information such as the ability to optimize tRNA affinity for elongation factor Tu (EF-Tu)¹⁵ (EF1A in eukaryotes), will facilitate the incorporation of desirable but recalcitrant unnatural residues into peptides and proteins.

Acknowledgment. This work was supported by NIH Grant (R01 60416) to R.W.R. and by NIH training Grant GM07616 (S.R.S.).

Supporting Information Available: Tricine-SDS-PAGE analysis of protein–puromycin products (Figure S1); model of D-puromycin–ribosome complex (Figure S2); experimental procedures (PDF). This material is available free of charge via the Internet at <http://pubs.acs.org>.

References

- (1) (a) Heckler, T. G.; Zama, Y.; Naka, T.; Hecht, S. M. *J. Biol. Chem.* **1983**, *258*, 4492–4495. (b) Bain, J. D.; Glabe, C. G.; Dix, T. A.; Chamberlin, A. R. *J. Am. Chem. Soc.* **1989**, *111*, 8013–8014. (c) Bain, J. D.; Wacker, D. A.; Kuo, E. E.; Chamberlin, A. R. *Tetrahedron* **1991**, *47*, 2389–2400.
- (2) (a) Noren, C. J.; Anthony-Cahill, S. J.; Griffith, M. C.; Schultz, P. G. *Science* **1989**, *244*, 182–188. (b) Nowak, M. W.; Kearney, P. C.; Sampson, J. R.; Saks, M. E.; Labarca, C. G.; Silverman, S. K.; Zhong, W.; Thorson, J.; Abelson, J. N.; Davidson, N.; Schultz, P. G.; Dougherty, D. A.; Lester, H. A. *Science* **1995**, *268*, 439–442.
- (3) (a) Li, S.; Millward, S.; Roberts, R. W. *J. Am. Chem. Soc.* **2002**, *124*, 9972–9973. (b) Takahashi, T. T.; Austin, R. J.; Roberts, R. W. *Trends Biochem. Sci.* **2003**, *28*, 159–165.
- (4) (a) Ellman, J.; Mendel, D.; Anthony-Cahill, S.; Noren, C. J.; Schultz, P. G. *Methods Enzymol.* **1992**, *202*, 301–336. (b) Hecht, S. M. *Acc. Chem. Res.* **1992**, *25*, 545–552. (c) Cornish, V. W.; Mendel, D.; Schultz, P. G. *Angew. Chem., Int. Ed. Engl.* **1995**, *34*, 621–633. (c) Gillmore, M. A.; Steward, L. E.; Chamberlin, A. R. *Top. Curr. Chem.* **1999**, *202*, 77–99. (d) van Hest, J. C. M.; Tirrell, D. A. *Chem. Commun.* **2001**, *19*, 1897–1904.
- (5) (a) Yamane, T.; Miller, D. L.; Hopfield, J. J. *Biochemistry* **1981**, *20*, 7059–7064. (b) Chládek, S.; Sprinzl, M. *Angew. Chem., Int. Ed. Engl.* **1985**, *24*, 371–391. (c) Heckler, T. G.; Roesser, J. R.; Xu, C.; Chang, P.-I.; Hecht, S. M. *Biochemistry* **1988**, *27*, 7254–7262. (d) Roesser, J. R.; Xu, C.; Payne, R. C.; Surratt, C. K.; Hecht, S. M. *Biochemistry* **1989**, *28*, 5185–5195.
- (6) Mendel, D.; Ellman, J.; Schultz, P. G. *J. Am. Chem. Soc.* **1993**, *115*, 4359–4360.
- (7) (a) Killian, J. A.; Van Cleve, M. D.; Shayo, Y. F.; Hecht, S. M. *J. Am. Chem. Soc.* **1998**, *120*, 3032–3042. (b) Koh, J. T.; Cornish, V. W.; Schultz, P. G. *Biochemistry* **1997**, *36*, 11314–11322. (c) Eisenhauer, B. M.; Hecht, S. M. *Biochemistry* **2002**, *41*, 11472–11478. (d) England, P. M.; Zhang, Y.; Dougherty, D. A.; Lester, H. A. *Cell* **1999**, *96*, 89–98.
- (8) Nathans, D. *Proc. Natl. Acad. Sci. U.S.A.* **1964**, *51*, 585–592.
- (9) (a) Fahnestock, S.; Neumann, H.; Shashoua, V.; Rich, A. *Biochemistry* **1970**, *9*, 2477–2483. (b) Gooch, J.; Hawtrey, A. O. *Biochem. J.* **1975**, *149*, 209–220. (c) Nathans, D.; Neidle, A. *Nature* **1963**, *197*, 1076–1077. (d) Harris, R. J.; Hanlon, J. E.; Symons, R. H. *Biochim. Biophys. Acta* **1971**, *240*, 244–262.
- (10) Campuzano, S.; Modolell, J. *Proc. Natl. Acad. Sci. U.S.A.* **1980**, *77*, 905–909.
- (11) Starck, S. R.; Roberts, R. W. *RNA* **2002**, *8*, 890–903.
- (12) Nissen, P.; Hansen, J.; Ban, N.; Moore, P. B.; Steitz, T. A. *Science* **2000**, *289*, 920–930.
- (13) Polacek, N.; Gaynor, M.; Yassin, A.; Mankin, A. S. *Nature* **2001**, *411*, 498–501.
- (14) (a) Krayevsky, A. A.; Kukhanova, M. K. *Prog. Nucleic Acids Res.* **1979**, *23*, 2–51. (b) Bhuta, P.; Kumar, G.; Chládek, S. *Biochim. Biophys. Acta* **1982**, *696*, 208–211.
- (15) (a) LaRiviere, F. J.; Wolfson, A. D.; Uhlenbeck, O. C. *Science* **2001**, *294*, 165–168. (b) Asahara, H.; Uhlenbeck, O. C. *Proc. Natl. Acad. Sci. U.S.A.* **2002**, *99*, 3499–3504.

JA034817E

Supporting Information

The Puromycin Route to Assess Stereo- and Regiochemical Constraints on Peptide Bond Formation in Eukaryotic Ribosomes

Shelley R. Starck, Xin Qi, Brett N. Olsen, and Richard W. Roberts*

Division of Chemistry and Chemical Engineering,

California Institute of Technology, Pasadena, CA 91125

General Information. ^1H and ^{13}C NMR spectra were recorded on a Varian, Inc. UNITY INOVA instrument operating at 500 MHz using D_2O or $\text{DMSO-}d_6$ as the solvent. ^1H NMR data are reported as follows: s, singlet; d, doublet; t, triplet; q, quartet; m, multiplet; br s, broad singlet; dd, doublet of doublets. High-resolution mass spectra (FAB) were recorded on a JMS-600H double-focusing, high-resolution, magnetic sector mass spectrometer at the Mass Spectrometry Laboratory, Division of Chemistry and Chemical Engineering, California Institute of Technology. Column chromatography was carried out on silica gel (40-63 μm , EM Science). Analytical HPLC was performed using a Vydac C18 column (5 mm, 4.5 x 250 mm) with buffer A (5 mM NH_4OAc , pH 5.5 with 10% acetonitrile) and buffer B (5 mM NH_4OAc , pH 5.5 with 90% acetonitrile); a linear gradient of 100% buffer B in 50 min was used with a flow rate of 1 mL/min. All reagents were of highest available commercial quality and were used without further purification. Puromycin aminonucleoside (3'-amino-3'-deoxy-*N,N'*-dimethyl-adenosine) (PANS) was purchased from Sigma Chemical Co. Fmoc-(4-methoxy-D-phenylalanine) and Fmoc-(D-alanine) were purchased from Bachem. Fmoc-(4-methyl-L-phenylalanine), Fmoc-(L-alanine), and Fmoc-(L- β -homoalanine) were purchased from Fluka. Fmoc-(4-

methyl-D-phenylalanine) and Fmoc-(4-methyl-L- β -phenylalanine) were from Peptech. Puromycin and puromycin analog concentrations were determined with the following extinction coefficients ($M^{-1}cm^{-1}$) at 260 nm: L- and D-puromycin (**1a** and **1b**) [$\epsilon = 11,790$] in H_2O ; L-(4-Me)-Phe-PANS, D-(4-Me)-Phe-PANS, and L- β -(4-Me)-Phe-PANS (**2a – 2c**) [$\epsilon = 10,500$] in H_2O ; and L-Ala-PANS, D-Ala-PANS, and L- β -Ala-PANS (**3a – 3c**) [$\epsilon = 11,000$] in phosphate buffered saline (pH 7.3).

Rabbit reticulocyte lysate was purchased from Novagen. Rabbit globin mRNA was obtained from Life Technologies Gibco BRL. L-Puromycin (**1a**) was purchased from Sigma Chemical Co. Ras mRNA was prepared by using two DNA primers complementary to the 5'- and 3'-ends of the coding region for H-Ras (pProEX HTb vector, a kind gift from Dafna Bar-Sagi)¹ to amplify the gene using PCR. mRNA was produced by T7 runoff transcription² of the H-Ras DNA in the presence of RNasecure (Ambion) followed by gel purification via denaturing urea-PAGE and 'crush and soak' RNA isolation. L-[³⁵S]methionine (1,175 Ci/mmol) was purchased from NEN Life Science Products. Carboxypeptidase Y was obtained from Pierce. GF/A glass microfiber filters were from Whatman. Scintillation counting was carried out using a Beckman LS-6500 liquid scintillation counter.

General Procedure for Preparation of Puromycin Analogs. *N, N'*-dicyclohexylcarbodiimide (DCC) (0.0539 mmol) was added to a cold (0 °C) solution of PANS (0.0520 mmol), Fmoc-protected amino acid (0.0541 mmol), and *N*-hydroxysuccinimide (NHS) (0.0556 mmol) in dried *N, N'*-dimethylformamide (DMF) (0.900 mL). The solution was stirred for 30 min in an ice-water bath and then for 25 h at ambient temperature. *N, N'*-dicyclohexylurea was filtered and washed (EtOAc, 4 mL),

and the filtrate was concentrated *in vacuo*. For **1b**, the residue was resuspended in EtOAc, sonicated, and the mixture was filtered and then dried. The material was purified by gradient flash chromatography using CHCl₃ → MeOH/CHCl₃ (4:96) for **1b** or MeOH/CHCl₃ (7:93) for **2a-2c** and **3a-3c**. Homogenous product fractions were dried *in vacuo* to yield the Fmoc-protected product. Fmoc-deprotection was carried out in 20% (v/v) piperidine in DMF (5mL) with stirring for 30 min at ambient temperature. The solvent was removed *in vacuo* and the residue was subjected to gradient flash chromatography using CHCl₃ → MeOH/CHCl₃ (8:92) for **1b**, **2a**, and **2b** and TEA/MeOH/CHCl₃ (2:10:88) for **2c** and **3a-3c** to afford the titled products. Confirmation of purity was assessed using analytical HPLC.

9-{3'-Deoxy-3'-[(4-methoxy-D-phenylalanyl)amino]-β-D-ribofuranosyl}-6-(N,N'-dimethylamino)purine (D-puromycin) (1b).³ White solid (31.5 mg, 87.3%): ¹H (DMSO-*d*6) δ 1.85 (br s, 2H), 2.58-2.63 (m, 1H), 2.93 (dd, *J* = 4.5, 14 Hz, 1H), 3.42 (dd, *J* = 4.5, 8.5 Hz, 2H), 3.51-3.56 (m, 2H), 3.72 (s, 6H), 3.93-3.96 (m, 1H), 4.47-4.51 (m, 4H), 5.17 (t, *J* = 5.5 Hz, 1H), 5.97 (d, *J* = 2.0 Hz, 1H), 6.17 (d, *J* = 5.0, 1H), 6.85 (d, *J* = 9.0 Hz, 2H), 7.15 (d, *J* = 8.5 Hz, 2H), 8.08 (br s, 1H), 8.24 (s, 1H), 8.45 (s, 1H); ¹³C (DMSO-*d*6) δ 25.4, 50.6, 56.0, 56.8, 61.7, 73.8, 84.4, 90.2, 114.3, 131.0, 138.7, 150.4, 152.6, 158.0, 175.5; HRMS (FAB), *m/z* calculated for C₂₂H₃₀N₇O₅ (M+H)⁺ 472.2311, found 472.2307.

9-{3'-Deoxy-3'-[(4-methyl-L-phenylalanyl)amino]-β-D-ribofuranosyl}-6-(N,N'-dimethylamino)purine [L-(4-Me)-Phe-PANS] (2a). Pale white solid (18.8 mg, 80.8%): ¹H NMR (DMSO-*d*6) δ 1.84 (br s, 2H), 2.26 (s, 6H), 2.52-2.57 (m, 1H), 2.94 (dd, *J* = 4.5, 14 Hz, 1H), 3.44-3.52 (m, 2H), 3.67-3.70 (m, 2H), 3.92-3.95 (m, 1H), 4.44-

4.50 (m, 4H), 5.14 (t, $J = 5.5$ Hz, 1H), 5.98 (d, $J = 3.0$ Hz, 1H), 6.14 (d, $J = 4.0$ Hz, 1H), 7.10 (dd, $J = 8.0, 18$ Hz, 4H), 8.07 (d, $J = 5.5$ Hz, 1H), 8.24 (s, 1H), 8.45 (s, 1H); ^{13}C (DMSO- d_6) δ 21.3, 41.2, 50.7, 56.9, 61.7, 73.9, 84.3, 90.2, 120.3, 129.4, 129.8, 135.7, 136.3, 138.7, 150.4, 152.6, 155.0, 175.5; HRMS (FAB), m/z calculated for $\text{C}_{22}\text{H}_{30}\text{N}_7\text{O}_4$ (M+H) $^+$ 456.2362, found 456.2367.

9-{3'-Deoxy-3'-[(4-methyl-D-phenylalanyl)amino]- β -D-ribofuranosyl}-6-(*N,N'*-dimethylamino)purine [D-(4-Me)-Phe-PANS] (2b). Pale white solid (20.7 mg, 88.8%): ^1H NMR (DMSO- d_6) δ 1.85 (br s, 2H), 2.26 (s, 6H), 2.61 (dd, $J = 8.0, 13$ Hz, 1H) 2.96 (dd, $J = 4.5, 14$ Hz, 1H), 3.42-3.45 (m, 1H), 3.51-3.56 (m, 1H), 3.71-3.73 (m, 2H), 3.94-3.96 (m, 1H), 4.40-4.49 (m, 4H), 4.48 (d, $J = 12$ Hz, 1H), 5.17 (t, $J = 5.5$ Hz, 1H), 5.97 (d, $J = 2.5$ Hz, 1H), 6.19 (br s, 1H), 7.11 (dd, $J = 8.0, 16$ Hz, 4H), 8.10 (br s, 1H), 8.23 (s, 1H), 8.45 (s, 1H); ^{13}C (DMSO- d_6) δ 21.4, 41.0, 50.6, 56.8, 61.7, 73.8, 84.4, 90.2, 120.3, 129.4, 129.9, 135.8, 136.1, 138.7, 150.4, 152.6, 155.0, 175.5; HRMS (FAB), m/z calculated for $\text{C}_{22}\text{H}_{30}\text{N}_7\text{O}_4$ (M+H) $^+$ 456.2362, found 456.2360.

9-{3'-Deoxy-3'-[(4-methyl-L- β -phenylalanyl)amino]- β -D-ribofuranosyl}-6-(*N,N'*-dimethylamino)purine [L- β -(4-Me)-Phe-PANS] (2c). Pale white solid (17.8 mg, 73.0%): ^1H NMR (D_2O) δ 2.06 (s, 6H), 2.45-2.49 (m, 1H), 2.67 (d, $J = 6.5$ Hz, 1H), 3.18 (t, $J = 6.0$ Hz, 1H), 3.28 (br s, 3H), 3.37-3.39 (m, 1H), 3.49-3.50 (m, 1H), 3.59-3.62 (m, 1H), 3.80 (dd, $J = 2.0, 13$ Hz, 1H), 4.08-4.10 (m, 1H), 4.35 (dd, $J = 6.0, 8.5$ Hz, 1H), 4.46 (dd, $J = 3.0, 5.5$ Hz, 1H), 5.94 (d, $J = 2.5$ Hz, 1H), 7.03 (s, 4H), 8.03 (s, 1H), 8.15 (s, 1H); ^{13}C NMR (D_2O) δ 19.1, 26.0, 40.5, 49.8, 50.5, 54.5, 60.8, 73.6, 82.7, 89.7, 111.0, 120.0, 129.4, 129.6, 134.0, 137.2, 138.0, 148.8, 152.3, 173.6; HRMS (FAB), m/z calculated for $\text{C}_{23}\text{H}_{32}\text{N}_7\text{O}_4$ (M+H) $^+$ 470.2519, found 470.2508.

9-{3'-Deoxy-3'-[(L-alanine)amino]-β-D-ribofuranosyl}-6-(N,N'-dimethylamino)purine (L-Ala-PANS) (3a). Pale yellow solid (5.7 mg, 30.2%): ¹H NMR (D₂O) δ 1.41 (d, *J* = 7.0 Hz, 3H), 3.28 (br s, 6H), 3.63 (dd, *J* = 3.5, 13 Hz, 1H), 3.82 (dd, *J* = 2.5, 13 Hz, 1H), 3.97 (q, *J* = 7.0 Hz, 1H), 4.17-4.18 (m, 1H), 4.55-4.58 (m, 2H), 4.62-4.64 (m, 1H), 5.98 (d, *J* = 3.0 Hz, 1H), 8.03 (s, 1H), 8.17 (s, 1H); ¹³C NMR (D₂O) δ 17.3, 39.0, 49.4, 51.0, 60.7, 73.5, 82.7, 89.6, 119.5, 138.0, 148.8, 152.2, 154.6, 172.4; HRMS (FAB), *m/z* calculated for C₁₅H₂₄N₇O₄ (M+H)⁺ 366.1892, found 366.1889.

9-{3'-Deoxy-3'-[(D-alanine)amino]-β-D-ribofuranosyl}-6-(N,N'-dimethylamino)purine (D-Ala-PANS) (3b). Pale yellow solid (8.6 mg, 45.4%): ¹H NMR (D₂O) δ 1.43 (d, *J* = 7.5 Hz, 3H), 3.28 (br s, 6H), 3.65 (dd, *J* = 4.0, 13 Hz, 1H), 3.83 (dd, *J* = 2.5, 13 Hz, 1H), 4.02 (q, *J* = 7.5 Hz, 1H), 4.14-4.17 (m, 1H), 4.55-4.58 (m, 2H), 4.64-4.66 (m, 1H), 5.98 (d, *J* = 3.0 Hz, 1H), 8.04 (s, 1H), 8.17 (s, 1H); ¹³C NMR (D₂O) δ 17.0, 39.0, 49.3, 50.9, 60.8, 73.3, 82.8, 89.6, 106.0, 119.6, 138.1, 152.3, 154.8, 172.0; HRMS (FAB), *m/z* calculated for C₁₅H₂₄N₇O₄ (M+H)⁺ 366.1892, found 366.1898.

9-{3'-Deoxy-3'-[(L-β-homoalanine)amino]-β-D-ribofuranosyl}-6-(N,N'-dimethylamino)purine (L-β-Ala-PANS) (3c). Pale yellow solid (4.6 mg, 25.6%): ¹H NMR (D₂O) δ 1.16 (d, *J* = 6.5 Hz, 3H), 1.74 (s, 1H), 2.52 (d, *J* = 3.5 Hz, 2H), 3.24 (br s, 6H), 3.52-3.61 (m, 2H), 3.78 (d, *J* = 13 Hz, 1H), 4.11 (d, *J* = 5.5 Hz, 1H), 4.62-4.64 (m, 2H), 5.93 (s, 1H), 7.99 (s, 1H), 8.13 (s, 1H); ¹³C NMR (D₂O) δ 18.2, 39.0, 39.5, 45.0, 50.7, 60.7, 73.5, 82.7, 89.6, 119.5, 138.0, 148.8, 152.2, 172.7; HRMS (FAB), *m/z* calculated for C₁₆H₂₆N₇O₄ (M+H)⁺ 380.2049, found 380.2054.

IC₅₀ Determination. Translation reactions containing [³⁵S]Met were made up in batch on ice and added in aliquots to microcentrifuge tubes containing an appropriate

amount puromycin or puromycin analog dried *in vacuo*. Typically, a 20 μL translation mixture consisted of 0.8 μL of 2.5 M KCl, 0.4 μL of 25 mM MgOAc, 1.6 μL of 12.5X Translation Mixture without methionine (25 mM dithiothreitol (DTT), 250 mM HEPES (pH 7.6), 100 mM creatine phosphate, and 312.5 μM of 19 amino acids, except methionine), 3.6 μL of nuclease-free water, 0.6 μL (6.1 μCi) of [^{35}S]Met (1175 Ci/mmol), 8 μL of Red Nova[®] nuclease-treated lysate, and 5 μL of 0.05 $\mu\text{g}/\mu\text{L}$ globin mRNA. Inhibitor, lysate preparation (include all components except template), and globin mRNA were mixed simultaneously and incubated at 30 °C for 60 min. Then 2 μL of each reaction was combined with 8 μL of tricine loading buffer (80 mM Tris-Cl (pH 6.8), 200 mM DTT, 24% (v/v) glycerol, 8% sodium dodecyl sulfate (SDS), and 0.02 % (w/v) Coomassie blue G-250), heated to 90 °C for 5 min, and applied entirely to a 4% stacking portion of a 16% tricine SDS-polyacrylamide gel containing 20% (v/v) glycerol⁴ (30 mA for 1.5h). Gels were fixed in 10% acetic acid (v/v) and 50% (v/v) methanol, dried, exposed overnight on a PhosphorImager screen, and analyzed using a Storm PhosphorImager (Molecular Dynamics). Analysis in Figure S1 was carried out as described above except 6 μL of each reaction and 24 μL of tricine loading buffer were loaded (1.5-fold increase in stacking and resolving portion of gel; 30mA for 7 h).

Carboxypeptidase Assay. Translation reactions were prepared as described for IC₅₀ determination except reactions (50 μL) contained 2 μL of 2.5 M KOAc, 1 μL of 25 mM MgOAc, 4 μL of 12.5X Translation Mixture without methionine (25 mM dithiothreitol (DTT), 250 mM HEPES (pH 7.6), 100 mM creatine phosphate, and 312.5 μM of 19 amino acids, except methionine), 16 μL (163 μCi) of [^{35}S]Met (1175 Ci/mmol), 20 μL of Red Nova[®] nuclease-treated lysate, and 6.96 μL of 230 $\mu\text{g}/\text{mL}$ Ras mRNA.³

Inhibitor, lysate components, and Ras mRNA were mixed simultaneously and incubated at 30 °C for 60 min. Then 2 µL of reaction was combined with 150 µL of 0.1 M sodium acetate (pH 5.0) and 17 µL carboxypeptidase Y (CPY) (1 mg/mL in 0.05 M sodium citrate (pH 5.3) Pierce), and incubated at 37 °C for 18 h. After incubation, reactions were mixed with 100 µL of 1 N NaOH/2% H₂O₂ (hydrolyzes charged tRNAs and removes the red color that may quench scintillation counting) and incubated at 37 °C for 10 min to hydrolyze the charged tRNAs. Then 0.9 mL of 25% trichloroacetic acid (TCA)/2% casamino acids was added to the samples, vortexed, and put on ice for 10 min. The samples were filtered on GF/A filters (pre-soaked in 5% TCA), washed 3 times with 3-mL portions of cold 5% TCA, and scintillation counted to determine the amount of [³⁵S]Met-Ras. For the no CPY-treated samples, [³⁵S]Met-Ras (2 µL of reaction) was TCA precipitated without CPY treatment as described above.

References

- (1) Boriack-Sjodin, P. A.; Margarit, S. M.; Bar-Sagi, D.; Kuriyan, J. *Nature* **1998**, *395*, 337-343. pProEX HTb vector (Gibco BRL) containing H-Ras (residues 1-166) linked to an N-terminal polyhistidine tag.
- (2) Milligan, J. F.; Uhlenbeck, O. C. *Methods Enzymol.* **1989**, *180*, 51-62.
- (3) Robins, M. J.; Miles, R. W.; Samano, M. C. *J. Org. Chem.* **2001**, *66*, 8204-8210.
- (4) Schagger, H.; Jagow, G. V. *Anal. Biochem.* **1987**, *166*, 368-379.

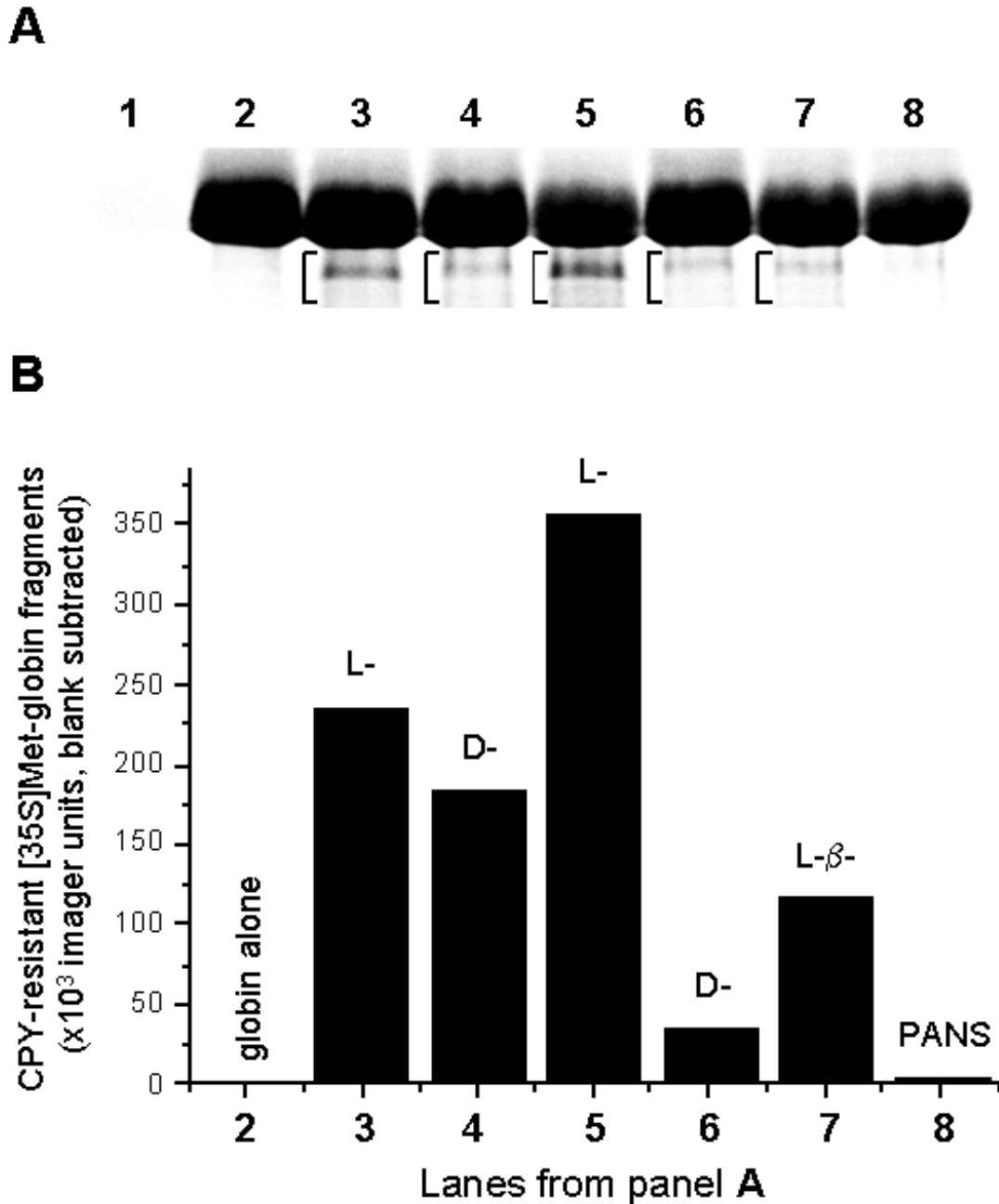


Figure S1. (A) Tricine-SDS-PAGE analysis of globin fragments resulting from puromycin and puromycin analog attachment. Lane 1, no template; lane 2, globin alone, no puromycin; lane 3, L-puromycin (2 μ M); lane 4, D-puromycin (500 μ M); lane 5, L-(4-Me)-Phe-PANS (2 μ M); lane 6, D-(4-Me)-Phe-PANS (1500 μ M); lane 7, L- β -(4-Me)-Phe-PANS (1200 μ M); lane 8, puromycin aminonucleoside (PANS) (5 mM). PANS is a negative control molecule (no amino acid moiety) to evaluate the production of protein fragments in the presence of high exogenous molecule concentrations. The globin fragment-puromycin complexes are indicated by brackets. (B) Quantification of the globin fragment-puromycin complexes from A.

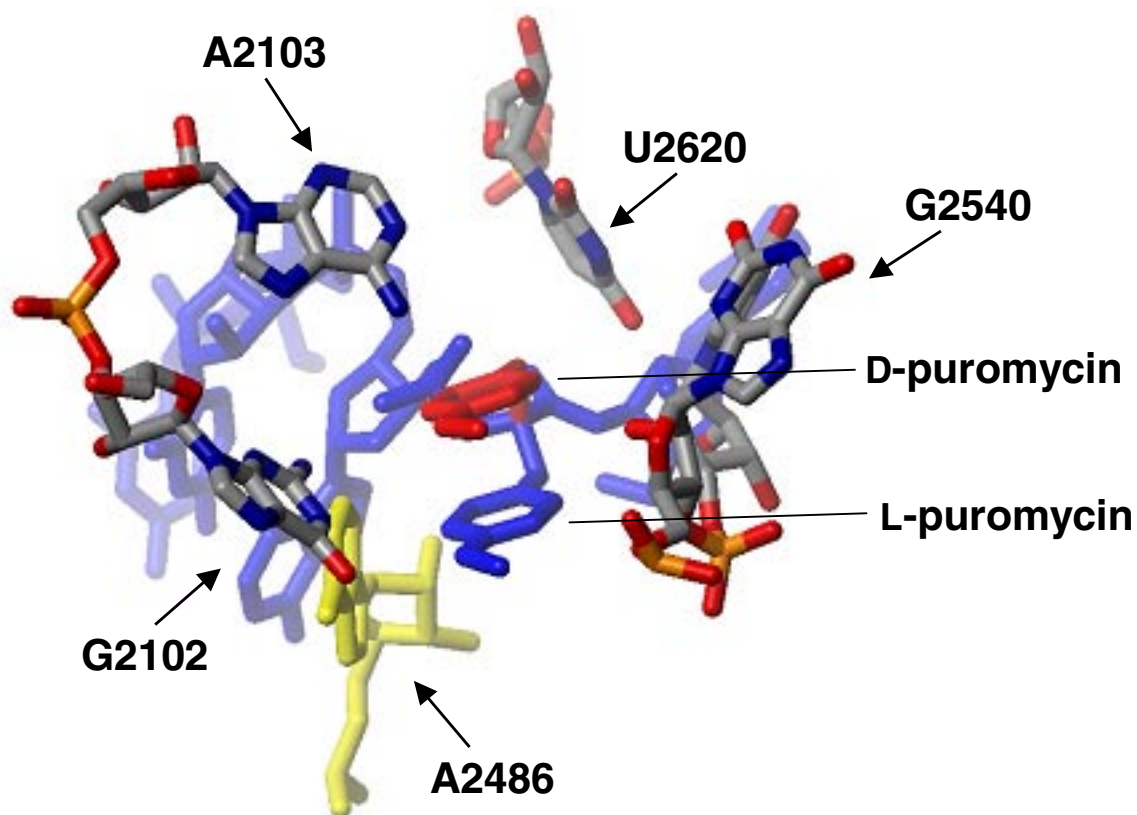


Figure S2. Model for D-puromycin (red) placement in the 50S ribosomal-CCdA-p-L-puromycin (blue) complex from *Haloarcula marismortui* (Nissen, P.; Hansen, J.; Ban, N., Moore, P. B.; Steitz, T. A. *Science* **2000**, 289, 920-930; PDB identifier 1FFZ). U2620 (U2585 in *Escherichia coli*) is the closest nucleotide to the D-puromycin side chain that may cause steric clash. A2486 (A2451 in *E. coli*) (yellow), the base possibly involved in peptidyl transferase catalysis, is shown for reference. G2102 (G2481), A2103 (A2482), and G2540 (G2505) are the next closest nucleotides ($\sim 5\text{\AA}$) to the D-puromycin side chain.